


Dynamic crossover towards energy equipartition in the Fermi-Pasta-Ulam-Tsingou β model with long-range interactions

Jian Wang * and Ai-chen Li*College of Physical Science and Technology, Yangzhou University, Yangzhou 225002, People's Republic of China*

(Received 23 February 2022; accepted 30 June 2022; published 25 July 2022)

Energy equipartition can be established in short-range systems after the dynamic process of thermalization. However, energy distribution between different degrees of freedom in systems with long-range interactions is unclear. We study the dynamics of energy relaxation in the Fermi-Pasta-Ulam-Tsingou β model with long-range quartic interactions, which decay as $1/d^\delta$ with d being the lattice distance. The dynamic crossover of a mode-energy distribution from localized to equipartitioned with the increase of the power δ is observed. A transition of mode-energy distribution is identified around the value of $\delta = 1$, which usually serves as the distinction between strong and weak long-range couplings. We elucidate that the varying frequency overlapping of the mode-energy power spectrum is responsible for this dynamic crossover. Through further calculation of the spectral entropy, the minimum duration of quasistationary states, τ_{QSS} , is found at $\delta = 2$, which may provide possible dynamic explanations for the peculiar behavior of heat transport in long-range lattice chains. In addition, the double scaling in τ_{QSS} as a function of energy density is also observed in our long-range lattices. Our results not only contribute to understanding the dynamics of energy relaxation in long-range systems, but also shed light on the longstanding problem of thermalization and low-dimensional heat transport in short-range systems.

DOI: [10.1103/PhysRevE.106.014135](https://doi.org/10.1103/PhysRevE.106.014135)

I. INTRODUCTION

As one of the central concepts of thermodynamics, energy equipartition hypothetically states that energy will be equally shared among all degrees of freedom in classical systems in thermal equilibrium. Studies of the underlying dynamic processes of energy equipartition can be traced back to the pioneering numerical experiments [1,2] by Fermi, Pasta, Ulam, and Tsingou (FPUT), where a peculiar recurrent behavior was observed instead of energy equipartition. Since then, extensive investigations in the FPUT nonlinear lattices have shown that energy equipartition can be reached above an energy threshold [3–7] or is slowly achieved through a metastable stage with varying equipartition time [7–18], depending on the energy density, nonlinear coupling strength, etc. In general, the process in which the system achieves thermal equilibrium with energy equipartition is referred to as thermalization. Other extrinsic factors such as disorder [19,20] and pressure [21] can affect the process of thermalization.

Long-range interactions [22–25] are present at various scales in nature, ranging from astrophysics [26,27] to atomic scales such as cold atoms [28] and quantum spin system [29–32]. As a result of the violation of additivity [22–25] in systems with long-range interactions, both the thermodynamic and dynamic properties of these systems are very different from the traditional Gibbs statistical physics with short-range interactions. For example, these thermodynamic features of long-range interactions include negative specific heat [33–36], ensemble inequivalence [37], non-Maxwellian momentum distributions [38–40], quasistationary

states [41–45] during the dynamical evolution, and the exotic heat transport properties [46–51]. Long-range interactions manifest [52] between either the internal or the external degrees of freedom of the particles and may lead to different behaviors of energy relaxation and distributions. The problem of how energies are distributed among normal modes in systems with long-range interactions is an interesting problem, but is rarely studied [53–57].

In this work, we take the Fermi-Pasta-Ulam-Tsingou (FPUT)- β model with the power-law decaying nonlinear interactions as an example to study energy relaxation and distribution in long-range systems. We find that the dynamic crossover of the mode-energy distribution from localized to equipartitioned can be observed, as the power exponent δ increases. Using the spectral entropy, we further study the effects of long-range interactions on the duration of quasistationary states (QSS) during energy relaxation. Our findings contribute to understanding the dynamic process of energy relaxation in the long-range system and may also shed light on the longstanding problem of thermalization and low-dimensional heat transport in short-range systems. The paper is organized as follows. In Sec. II, we first introduce the model and describe the adopted numerical methods during calculations. In Sec. III, we then present our main results of energy relaxation and distribution in the long-range system. Finally, conclusions and remarks are made in Sec. IV.

II. MODELS AND METHODS

A. Models

We consider the long-range FPUT- β model with the power-law decaying nonlinear interactions with periodical boundary

*phcwj@hotmail.com

conditions. The Hamiltonian is given by

$$H = \sum_{i=1}^N \left[\frac{p_i^2}{2m_i} + \frac{1}{2}(q_{i+1} - q_i)^2 + \frac{1}{4\tilde{N}} \sum_{j=1, j \neq i}^N \frac{(q_i - q_j)^4}{|d_{ij}|^\delta} \right], \quad (1a)$$

$$\tilde{N} = \frac{1}{N} \sum_{i=1}^N \sum_{j=1, j \neq i}^N |d_{ij}|^{-\delta}, \quad (1b)$$

where p_i and q_i denote the momentum and displacement of the i th particle with mass m_i , which has been set to one for convenience. Here, i, j are the lattice sites and also correspond to the indices of particles on the lattice sites, respectively. $d_{ij} = 1, 2, 3, \dots$ is the shortest distance between the i, j th lattice sites under periodical boundary conditions. N is the total number of particles considered. The prefactor with \tilde{N} in the quartic potential energy of Hamiltonian (1) is introduced in order to yield [58] the extensive total energy. Compared with the generalized mean-field Hamiltonian with long range interactions [24,25], the present long-range interactions are included in the quadratic part of Hamiltonian (1), which has the power-law decrease with lattice distant $d_{ij}^{-\delta}$. There are two limits: (i) $\delta \rightarrow 0$ means that each particle interacts equally with other particles, independent of the distance between them, which is similar to the mean-field Hamiltonian [24,25]; (ii) $\delta \rightarrow \infty$ corresponds to the nearest-neighbor non-linear interaction, recovering the Hamiltonian of the historical FPUT- β model. In the work, we concentrate on the FPUT- β model with only long-range quartic interactions since most of the interesting dynamic behaviors of long-range systems can be obtained [55,57,59] in the present model. For example, a decrease of the largest Lyapunov exponent with system size [55,59] and q -statistics of velocity distributions [57,59] has been observed in the present model when $\delta < 1$. The peculiar behavior of heat transport is also observed [46–51] in the present model.

B. Methods

Fourier transform of momentum and displacement should be adopted since energy partition is investigated in terms of normal modes. Under the periodical boundary conditions, i.e., $q_N = q_0$, we take the following Fourier transform of the momentum p_i and displacement q_i :

$$Q_k = \frac{1}{N} \sum_{j=0}^{N-1} q_j e^{-i2\pi k j/N}, \quad P_k = \frac{1}{N} \sum_{j=0}^{N-1} p_j e^{-i2\pi k j/N}, \quad (2)$$

where $k = 0, \dots, N - 1$ are discrete wave numbers, and Q_k and P_k are the amplitudes of displacement and momentum in the Fourier space. The angular frequency ω_k and the harmonic energy E_k of the k th normal mode are then expressed, respectively, as

$$\omega_k = 2|\sin(k\pi/N)|, \quad E_k(t) = \frac{1}{2}(\omega_k^2 Q_k^2 + P_k^2). \quad (3)$$

To describe the varying normal-mode energy distribution up to time t , the time average mode energy [11,13] $\bar{E}_k(t)$ is

calculated in the running time window $\mu t \leq s \leq t$ by

$$\bar{E}_k(t) = \frac{1}{(t - \mu t)} \int_{\mu t}^t E_k(s) ds. \quad (4)$$

In our calculations, the time window μ is set as $\mu = 2/3$. According to the principle of energy equipartition, we can expect that $\bar{E}_k(t \rightarrow \infty) \simeq \epsilon$, where ϵ is the constant energy density for each normal mode.

Based on the calculation of $\bar{E}_k(t)$ in Eq. (4), the spectral entropy $s(t)$ can be introduced [3,4,14],

$$s(t) = \sum_{k=1}^{N-1} f_k(t) \ln f_k(t), \quad f_k(t) = \frac{N-1}{\sum_{j=1}^{N-1} \bar{E}_j(t)} \bar{E}_k(t). \quad (5)$$

Here we have used $N - 1$ instead of N because the first mode $k = 0$ is not involved in the dynamics under periodical boundary conditions. When the state of energy equipartition is reached, the value of spectral entropy is theoretically zero. To measure the dynamic process towards energy equipartition quantitatively, the normalized effective relative number of the degrees of freedom [4] can be defined,

$$n(t) = \frac{e^{\xi(t)}}{N-1}, \quad \xi(t) = - \sum_{k=1}^{N-1} w_k(t) \ln w_k(t), \quad (6)$$

with the normalized spectral entropy given by $w_k(t) = f_k(t)/(N - 1)$. Therefore, the energy relaxation process of normal modes can be dynamically characterized by the normalized effective relative number $n(t)$, where $n(t) = 1$ theoretically for the state of energy equipartition. The values of $s(t)$ and $n(t)$ generally depend on the initial configures of the normal modes if equipartition is not reached.

In our simulations, the velocity-Verlet algorithm is adopted for integrating the motion equations with the time step, $h = 0.125$. The energy conservation with the relative accuracy of about 10^{-4} is checked for energy fluctuation during the simulation. Because of the heavy computations, we employ the graphics processing unit (GPU) to implement the parallel acceleration of molecular dynamics simulation and the Fourier transform. To overcome fluctuations statistically, the value of spectral entropy $s(t)$ and the normalized effective relative number $n(t)$ have been further averaged over more than 10 realizations of random initial velocities during our calculations.

III. RESULTS AND DISCUSSIONS

We systematically explore energy relaxation for the long-range FPUT- β model in Eq. (1) with different values of the decaying power δ . To focus on the effect of long-range coupling, the length of the FPUT- β chain is fixed during our simulations. We first present the distribution of energies along normal modes and then investigate the time duration of quasi-stationary states for the energy relaxation process.

A. Distributions of energies of normal modes

The energy distributions along normal modes at time step $t = 0, 10^5$, and 10^8 for the long-range FPUT- β models with the power-law decaying coefficient $\delta = 0, 2, 8$ are shown in Figs. 1(a), 1(b) and 1(c), respectively. To describe how the system nontrivially interpolates between the initial condition

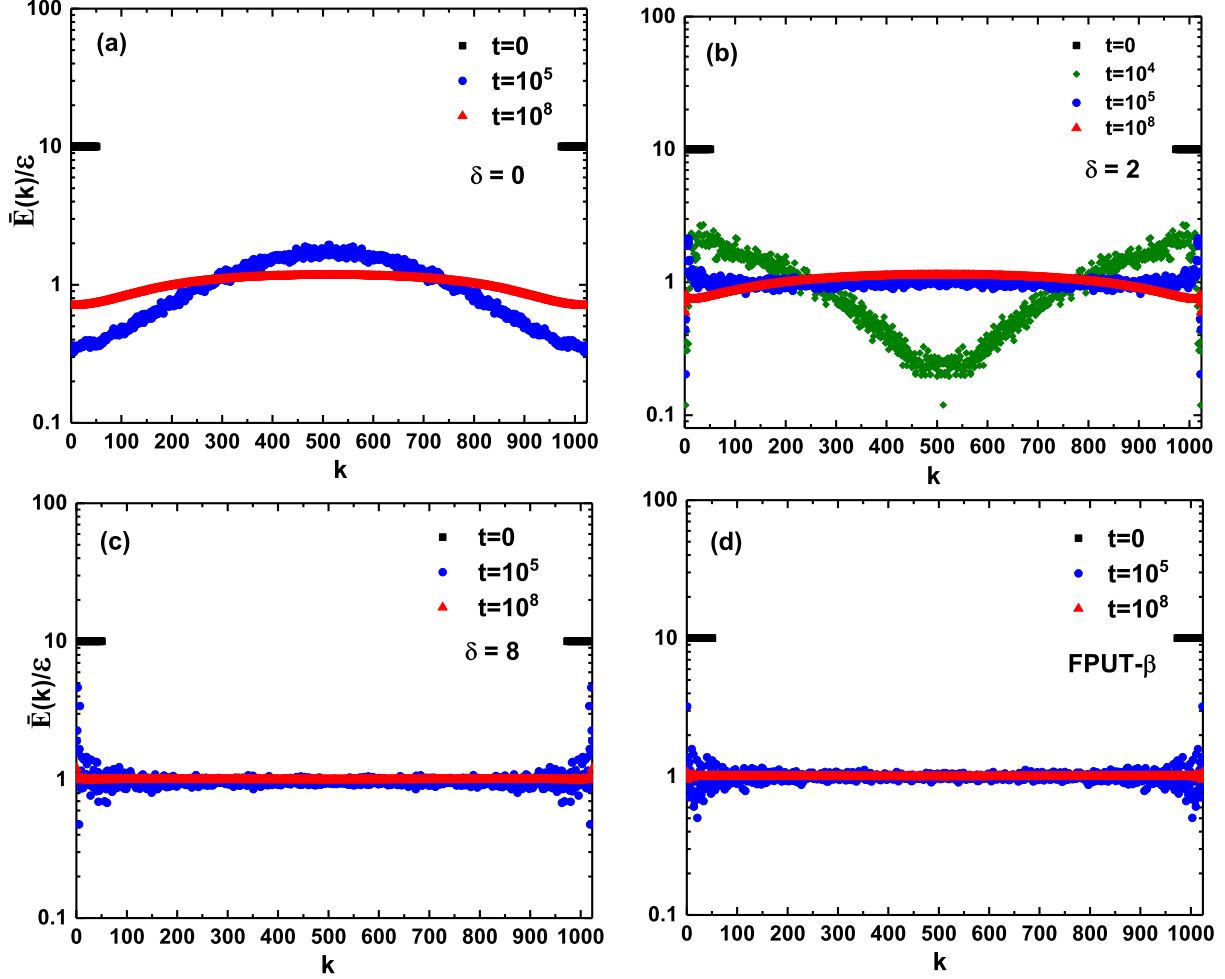


FIG. 1. The energy distributions along normal modes at different times for the long-range FPUT- β models with different power-law decaying coefficient δ : (a) $\delta = 0$, (b) $\delta = 2.0$, (c) $\delta = 8.0$, (d) $\delta = \infty$ (i.e., the nearest FPUT- β model). The time is indicated in each figure. The initially excited lowest and highest modes at $t = 0$ are indicated by the black square. The energy density is set to $\epsilon = 0.5$ and the chain length $N = 1024$.

and the long-time solution at $\delta = 2$, the curve at $t = 10^4$ is also plotted in Fig. 1(b). For comparison, the energy distribution for the nearest-neighbor FPUT- β model is plotted in Fig. 1. In order to better show the process of energy relaxation, only the lowest and highest modes are initially excited at $t = 0$, as indicated by the black square in the figures. As the system evolves, the energies of initially excited modes spread to other normal modes owing to the nonlinear interactions. The blue circle and red triangle in the figures correspond to the energy distributions at time step $t = 10^5$ and $t = 10^8$, respectively. Our longer time simulations give similar results as that of $t = 10^8$ in the figure. Therefore, the energy distribution at time $t = 10^8$ can be treated as the steady state. It can be seen from Fig. 1 that the energies of normal modes gradually tend to be equally distributed with the increase of the coefficient δ . We can clearly find that the distributions of normal energies vary from localized for the long-range coupling to equipartitioned for the nearest-neighbor coupling. To demonstrate the crossover of mode-energy distribution explicitly, a comparison of the steady distributions of mode energies at time step $t = 10^8$ for the FPUT- β models with the

various coefficient δ is further plotted in Fig. 2. It can be seen from Fig. 2(a) that the curves of mode-energy distribution almost coincide for $\delta = 0$ and 1, where a strong long-range interaction [24] can be assumed. We can find that energy in the Fourier space is strongly localized during the regime $\delta \leq 1$. This localization behavior of normal modes may possibly be related to the nonergodicity characterized [55,60] by the vanishing value of the maximal Lyapunov exponent with system size N . In the weak long-range coupling [24] regime of $\delta > 1$, the energy distribution along normal modes gradually tends to be flattened as δ increases, possibly resulting from the increased overlap of the power spectrum of normal modes in the following. Therefore, it can intuitively be expected from Fig. 2(a) that energy relaxation among normal modes is enhanced such that energy equipartition will be reached when $\delta \rightarrow \infty$. From Fig. 2(a), we may assume that the transition of the energy distribution for normal modes can be estimated around $\delta = 1$. To investigate the finite-length dependence of the energy distribution in the Fourier space, we have calculated the energy distribution at $\delta = 0$ with different lengths $N = 512, 1024, 4096$, respectively. The steady distributions

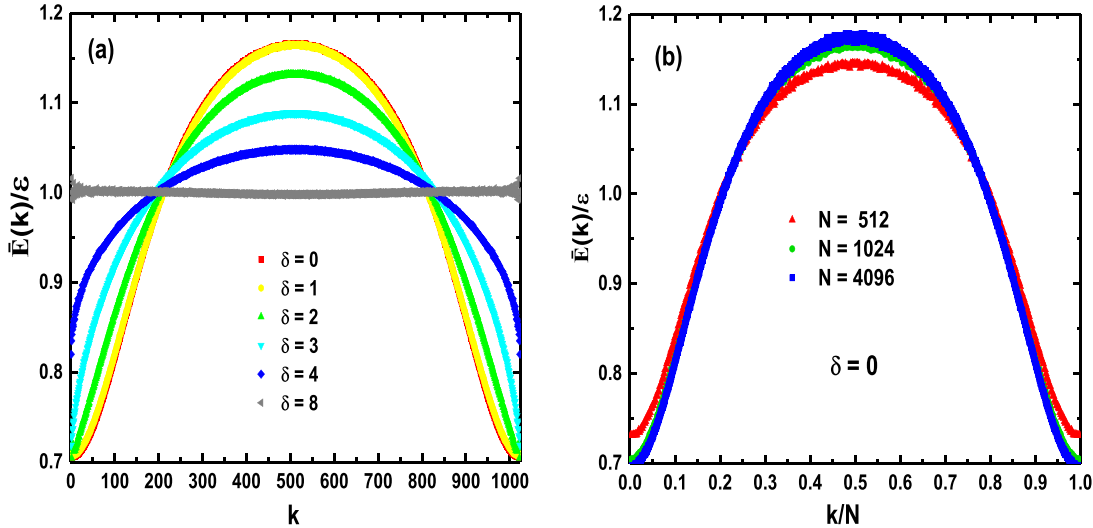


FIG. 2. (a) Comparison of the steady distributions of normal-mode energies for the FPUT- β models with different decaying power δ . The energy density is set to $\epsilon = 0.5$ and the chain length $N = 1024$. (b) The steady distributions of normal-mode energies for the long-range FPUT- β model ($\delta = 0$) with different lengths $N = 512, 1024$, and 4096 , respectively.

are shown in Fig. 2(b). We can find that the energy distribution tends to be more localized with the increase of N . However, the difference of energy distribution of normal modes between $N = 1024$ and $N = 4096$ is not very big. Therefore, we think that the length of $N = 1024$ may be a suitable choice as far as the heavy computations is concerned.

Furthermore, we expound the possible reasons for the crossover of energy distribution from localized to equipartitioned with the varying power δ . As for the short-range FPUT models, the energy relaxation to equipartition has been theoretically described [10,14,17,20] by the wave-turbulence approach in the weak-nonlinear limit. However, there is no theoretical approach to energy relaxation in the long-range FPUT models due to the complexity of long-range interactions. The energy transfer from one normal mode to other modes can be explained [17] by the resonant overlap of normal modes with nonlinear frequency broadening. In order to understand energy relaxation for the long-range FPUT- β models, we plot the power spectrum of different normal-mode energies with the various long-range coefficient δ in Fig. 3 as a function of frequency. Each spectrum of normal-mode energy $E(k, \omega)$ is obtained through the Fourier transform of a normal-mode energy $E_k(t)$ in Eq. (3) with time t after the steady state of the system is reached. It can be seen from Fig. 3 that high-frequency modes show quite different behaviors of frequency broadening from that of low-frequency modes as the long-rang power exponent δ increases. We can find that the frequency broadening of low-frequency modes decreases with increase of δ , as indicated by the black square and red circle in Fig. 3. On the contrary, the frequency broadening of high-frequency modes is strongly enhanced with increase of the long-range power exponent δ , as shown by the lines with the wave number such as $k = 15$ and 16 . in Fig. 3. Owing to the varying broadening of frequency with the power exponent δ , different overlapping of resonance occurs in the range of the low and high frequencies. For example, there is no noticeable overlapping of resonance between the power spectrum of low-frequency modes and that of high-frequency

modes for $\delta = 0.0$ and 1.0 at frequency about $\omega \simeq 0.75$, as shown in Figs. 3(a) and 3(b). This existence of a band gap between the high- and low-frequency power spectrum implies that there is a weak energy exchange between high and low modes such that energy is hard to be equally distributed, leading to localized distribution of energy along normal modes as shown in Figs. 1(a), 1(b), and 2 with $\delta = 0, 1$. Conversely, the overlap of the power spectrum between low and high frequencies is apparent in Figs. 3(c)–3(e) when the long-range power exponent $\delta \geq 2$. Therefore, the energy exchange between high- and low-frequency modes can be easily carried through the overlapping of the resonant power spectrum so that energy equipartition can be gradually approached with the increasing value of the long-range power exponent δ .

B. The duration of quasistationary states

Out of equilibrium, the relaxation to equilibrium of lattice systems with long-range pair interaction is characterized [41,43] by the existence of quasistationary states, which is similar to the metastable state [10,14,17] in short-range lattices during thermalization. We further investigate the time duration of quasistationary states for the long-range FPUT- β models with increasing values of power exponent δ .

As an indicator of thermalization, the spectral entropy $s(t)$ given by Eq. (5) measures the degree to which the energies of the entire system are equally distributed among normal modes. Theoretically, $s(t) = 0$ if energy equipartition is established for the system. The results of time evolution of spectral entropy $s(t)$ for the long-range FPUT- β models with different values of δ and for the nearest-neighbor FPUT- β model are shown in Fig. 4. To overcome fluctuations, the spectral entropy $s(t)$ as well as the normalized effective relative number $n(t)$ in the following has been averaged from more than 10 realizations of random initial velocities during our calculations. It can be observed from Fig. 4 that the spectral entropy $s(t)$ of the long-range interaction system with $\delta = 0, 1, 2, 3, 4$ first decreases and then tends to be stabilized as the relaxation time

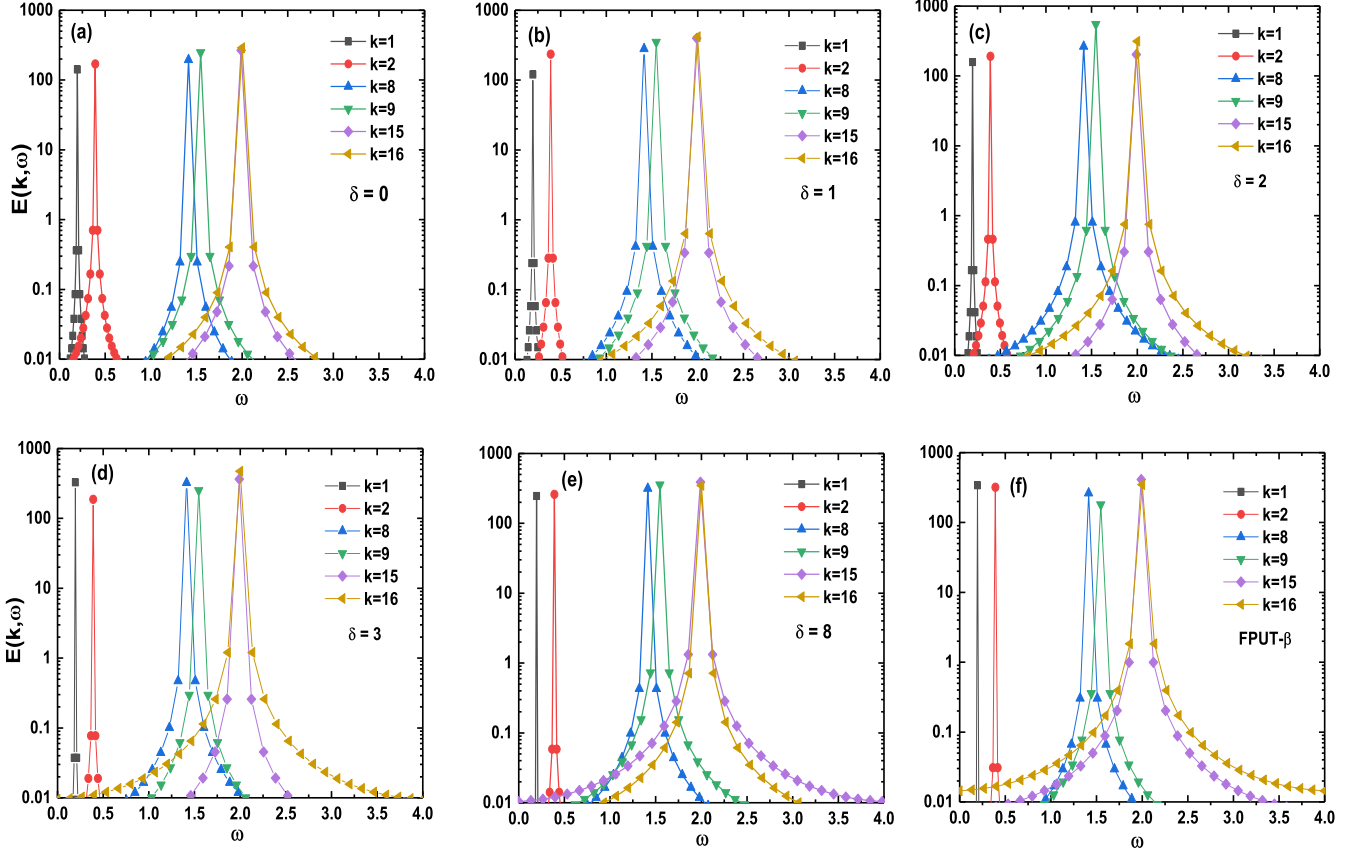


FIG. 3. Power spectrum of different normal-mode energies as a function of frequency for the long-range FPUT- β model with various power coefficient δ : (a) $\delta = 0$, (b) $\delta = 1$, (c) $\delta = 2$, (d) $\delta = 3$, (e) $\delta = 8$, (f) $\delta = \infty$, i.e., the short-range FPUT- β model. For brevity, the length of system N is set to $N = 32$ with the energy density of $\epsilon = 0.5$.

increases. The stabilized states correspond to the steady distributions of mode energy in Fig. 2. We can find that the value of stabilized $s(t)$ decreases with increase of the power exponent δ , implying the process of transition towards energy equipar-

tion. The stabilized values for $\delta = 0, 1$ coincide with each other after time $t > 10^7$, which is consistent with the result in Fig. 2. In addition, the spectral entropy $s(t)$ for the long-range FPUT- β with $\delta = 8$ collapses to that of the nearest-neighbor FPUT- β at small values, suggesting the crossover of normal-mode energy distribution towards equipartition.

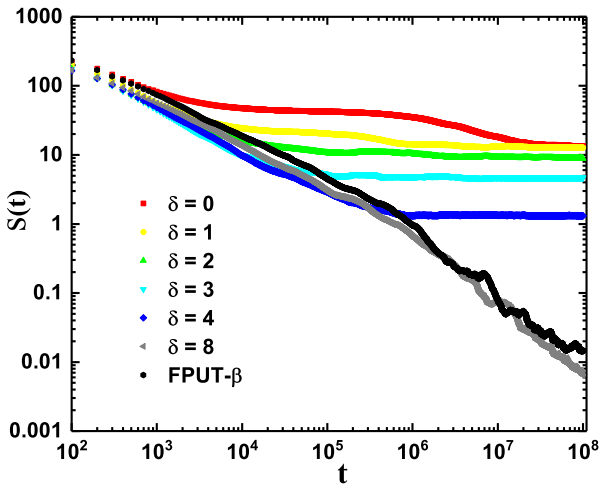


FIG. 4. The evolution of spectral entropy $s(t)$ as a function of time t for the long-range FPUT- β models with different values of power exponent $\delta = 0, 1, 2, 3, 4, 8$ and for the nearest-neighbor FPUT- β model. The length of lattice chain N is 1024 and the energy density $\epsilon = 0.5$.

Similar to the calculation of thermalization time [10,14,17] for short-range systems, we propose that the duration of quasi-stationary states τ_{QSS} can be further estimated from the normalized effective relative number $n(t)$ defined in Eq. (6). The time evolution of the normalized effective relative number $n(t)$ for the long-range FPUT- β models with the power exponent δ is plotted in Fig. 5(a). Energy equipartition theoretically corresponds to $n(t) = 1$. However, energy equipartition in the long-range FPUT- β models cannot be reached exactly so that a small value of deviation from the theoretical value of one exists, as shown in Fig. 5(a) after the time step of 10^7 . To estimate the duration time τ_{QSS} , we introduce a threshold n_{shr} of the normalized effective relative number $n(t)$. During our calculations, the threshold n_{shr} is taken as Cn_{max} , where n_{max} is the maximal value of the stabilized effective relative number $n(t)$. The threshold n_{shr} for each $n(t)$ with different power exponent δ is indicated by the vertical dashed lines in Fig. 5(a). Our approach to estimate the duration time τ_{QSS} is similar to the method to calculate thermalization time [11]. Because the choice of value C is highly arbitrary, we have numerically verified that the choice of different value

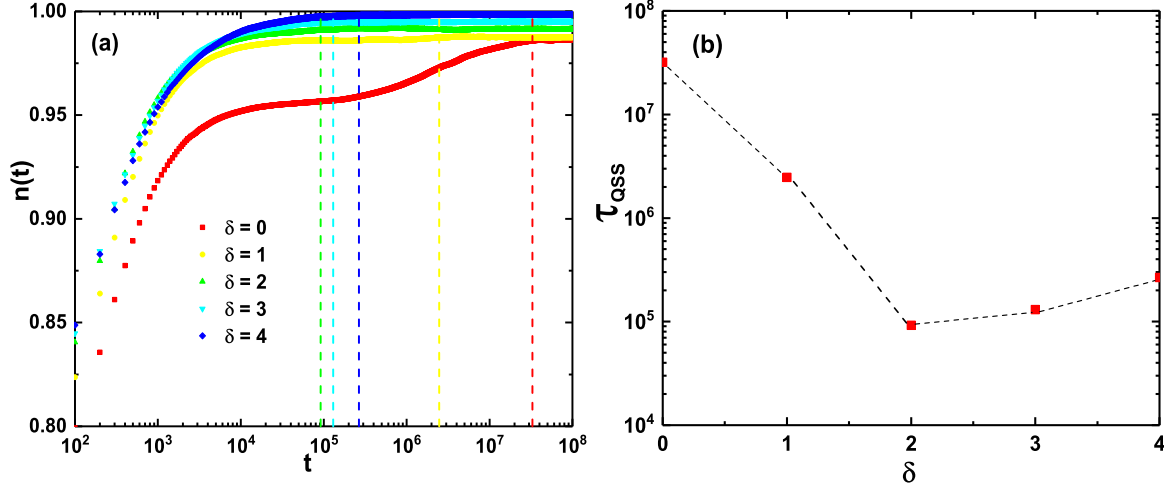


FIG. 5. (a) The time evolution of the normalized effective relative number $n(t)$ for the long-range FPUT- β models with the power exponent $\delta = 0, 1, 2, 3, 4$. The dashed lines indicate the positions of threshold with $n_{\text{shr}} = n_{\text{max}}$. The length of lattice chain N is 1024 and the energy density $\epsilon = 0.5$. (b) The duration of quasistationary states τ_{QSS} varying with the power-law decay exponent δ .

of the factor C in some broad range is insensitive to the estimation of the duration time τ_{QSS} . Note that the duration time τ_{QSS} of quasistationary states in long-range systems can also be estimated [38] by the transition of kinetic energy (temperature). Our approach is based on the transition of mode-energy distribution from localized to equipartitioned, while the method in Ref. [38] depends on the transition of velocity distribution from non-Maxwellian to Boltzmann-Gibbs. We think that both of the approaches may be essentially similar because the transition of either the mode-energy distribution or the velocity distribution is underlined by the change of the same intrinsic dynamics in long-range systems.

The calculated duration τ_{QSS} versus the long-range power exponent δ is shown in Fig. 5(b). Here, we focus the value of long-range power exponent δ around $\delta = 2$ because a puzzling ballisticlike heat transport is observed [48,50,51] in the long-range FPUT- β with $\delta = 2$. It can be observed from Fig. 5(b)

the duration τ_{QSS} has the minimum value at $\delta = 2$. We expect that this agrees with the fast heat diffusion [50] obtained from the spatiotemporal correlation of fluctuation function and with the ballisticlike heat transport [51] around $\delta = 2$. We have also verified a ballistic heat diffusion at $\delta = 2$ in our present models. The reason these two observations are consistent may lie in the fact that faster thermal diffusion around $\delta = 2$ may make normal modes reach the final steady state quickly.

We further explore the dependence of the duration of quasistationary states τ_{QSS} on energy density at $\delta = 2$. Comparison of the evolution of the normalized effective relative number $n(t)$ for the long-range FPUT- β models at $\delta = 2$ with different energy densities ϵ is plotted in Fig. 6(a). The calculated time duration τ_{QSS} as a function of energy density is given in Fig. 6(b) with the given threshold $n_{\text{shr}} = 0.95$, as indicated by the dashed lines. We can obviously

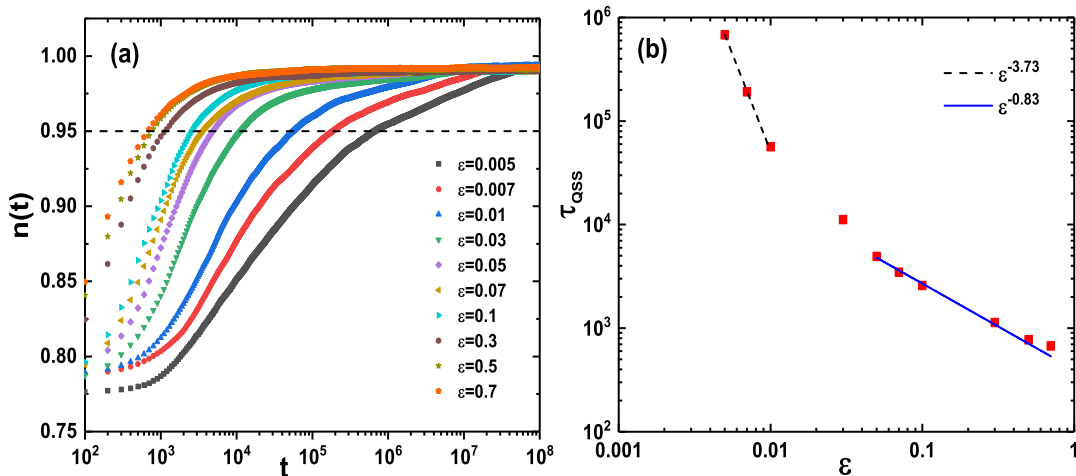


FIG. 6. (a) Comparison of the evolution of the normalized effective relative number $n(t)$ for the long-range FPUT- β models at $\delta = 2$ with different energy densities ϵ . The dashed lines indicate the positions of threshold, $n_{\text{shr}} = 0.95$. The length of lattice chain N is 1024. (b) The time duration of quasistationary states τ_{QSS} as a function of energy density with the power-law decay exponent $\delta = 2$. The square represents numerical simulations. The straight line corresponds to the fitted power law of $1/\epsilon^{3.73}$ (dashed line) and of $1/\epsilon^{0.83}$ (solid line), respectively.

observe the double scaling relationship $\tau_{\text{QSS}} \sim 1/\epsilon^{3.73}$ and $\tau_{\text{QSS}} \sim 1/\epsilon^{0.83}$, respectively. Similar behavior of double scaling in the relaxation time has been previously reported [17] in the nearest-neighbor FPUT- β model with the relation $\tau_{eq} \sim 1/\epsilon^4$ and $\tau_{eq} \sim 1/\epsilon^1$, respectively. We speculate that the mechanism behind both may be similar [17]: the steepest $\tau_{\text{QSS}} \sim 1/\epsilon^{3.73}$ at lower energy density results from the irreversible six-wave interactions, while the $\tau_{\text{QSS}} \sim 1/\epsilon^{0.83}$ at higher energy density is associated with the nonlinearity in the dynamical equation for the overlap over broadening frequency.

IV. CONCLUSIONS AND DISCUSSION

In summary, we have studied the dynamics of energy relaxation along normal modes in the long-range FPUT- β model with the power-law decaying quartic interactions. The dynamic crossover of energy distribution from localized to equipartitioned versus wave numbers k is clearly observed as the power exponent δ increases from 0 to ∞ , i.e., the nearest-neighbor FPUT- β . We show that the different frequency overlapping of the mode-energy power spectrum is responsible for the crossover of the energy distribution, since the frequency broadening of the high- and low-frequency energy modes varies with the long-range coupling power δ . Through further calculation of the spectral entropy, the minimum duration of quasistationary states (QSS) τ_{QSS} is found at $\delta = 2$, implying faster relaxation of the mode energies, which may provide possible dynamic explanations for the peculiar behavior of heat transport in long-range lattice chains. Similar

to that of the nearest-neighbor FPUT- β model, the double scaling in τ_{QSS} as a function of energy density is also observed in our long-range lattices.

Our results not only contribute to understanding the dynamics of energy relaxation in long-range systems, but also shed light on the longstanding problem of both thermalization and low-dimensional heat transport in short-range systems. Note that our present work is focused on the long-range FPUT- β model only with the long-range quartic interactions and the fixed system length. Actually, long-range interactions can be imposed either on the quadratic potential or on the quartic one, or on both simultaneously. The difference in dynamics and statistics for different ranges of long interaction has been discussed in Ref. [59], which suggests that more interesting dynamic phenomena appear in the FPUT- β model with the long-range quartic potential. We think that the reason may lie in the fact that the oscillation with only the long-range harmonic part can be transformed into the renormalized normal modes [56] so that the deviation of its dynamics from that of the nearest-neighbor FPUT- β is not large. Due to heavy computations, we leave the problem of energy relaxation with different conditions such as the long-range quadratic coupling and different energy densities for future pursuit.

ACKNOWLEDGMENTS

We thank Daxing Xiong for useful discussions. J.W. acknowledges the support from the National Natural Science Foundation of China (NSFC) under Grant No. 11875047.

-
- [1] E. Fermi, P. Pasta, S. Ulam, and M. Tsingou, Los Alamos Scientific Laboratory Report No. **LA-1940** (1955).
 - [2] G. Gallavotti, *The Fermi-Pasta-Ulam Problem: A Status Report*, Lecture Notes in Physics (Springer, Berlin, 2008).
 - [3] R. Livi, M. Pettini, S. Ruffo, and A. Vulpiani, *Phys. Rev. A* **31**, 2740 (1985).
 - [4] R. Livi, M. Pettini, S. Ruffo, M. Sparpaglione, and A. Vulpiani, *Phys. Rev. A* **31**, 1039 (1985).
 - [5] J. De Luca, A. J. Lichtenberg, and M. A. Lieberman, *Chaos* **5**, 283 (1995).
 - [6] L. Casetti, M. Cerruti-Sola, M. Pettini, and E. G. D. Cohen, *Phys. Rev. E* **55**, 6566 (1997).
 - [7] J. De Luca, A. J. Lichtenberg, and S. Ruffo, *Phys. Rev. E* **60**, 3781 (1999).
 - [8] F. Fucito, F. Marchesoni, E. Marinari, G. Parisi, L. Peliti, S. Ruffo, and A. Vulpiani, *J. Phys. France* **43**, 707 (1982).
 - [9] R. Livi, M. Pettini, S. Ruffo, M. Sparpaglione, and A. Vulpiani, *Phys. Rev. A* **28**, 3544 (1983).
 - [10] W. Fu, Y. Zhang, and H. Zhao, *Phys. Rev. E* **100**, 010101(R) (2019).
 - [11] G. Benettin and A. Ponno, *J. Stat. Phys.* **144**, 793 (2011).
 - [12] A. Ponno, H. Christodoulidi, C. Skokos, and S. Flach, *Chaos* **21**, 043127 (2011).
 - [13] G. Benettin, H. Christodoulidi, and A. Ponno, *J. Stat. Phys.* **152**, 195 (2013).
 - [14] M. Onorato, L. Vozella, D. Proment, and Y. V. Lvov, *Proc. Natl. Acad. Sci. USA* **112**, 4208 (2015).
 - [15] Z. Zhang, C. Tang, J. Kang, and P. Tong, *Chin. Phys. B* **26**, 100505 (2017).
 - [16] Z. Zhang, C. Tang, and P. Tong, *Phys. Rev. E* **93**, 022216 (2016).
 - [17] Y. V. Lvov and M. Onorato, *Phys. Rev. Lett.* **120**, 144301 (2018).
 - [18] W. Fu, Y. Zhang, and H. Zhao, *New J. Phys.* **21**, 043009 (2019).
 - [19] L. L. Sun, Z. J. Zhang, and P. Q. Tong, *New J. Phys.* **22**, 073027 (2020).
 - [20] Z. Wang, W. Fu, Y. Zhang, and H. Zhao, *Phys. Rev. Lett.* **124**, 186401 (2020).
 - [21] W. Fu, Y. Zhang, and H. Zhao, *Phys. Rev. E* **104**, L032104 (2021).
 - [22] T. Dauxois, *Dynamics and Thermodynamics of Systems with Long-range Interactions*, Lecture Notes in Physics (Springer, Berlin, 2002).
 - [23] A. Campa, T. Dauxois, and S. Ruffo, *Phys. Rep.* **480**, 57 (2009).
 - [24] A. Campa, T. Dauxois, D. Fanelli, and S. Ruffo, *Physics of Long-range Interacting Systems*, 1st ed. (Oxford University Press, Oxford, 2014).
 - [25] Y. Levin, R. Pakter, F. B. Rizzato, T. N. Teles, and F. P. C. Benetti, *Phys. Rep.* **535**, 1 (2014).
 - [26] T. Padmanabhan, *Phys. Rep.* **188**, 285 (1990).

- [27] S. Binney and James Tremaine, *Galactic Dynamics* (Princeton University Press, Princeton, NJ, 2008).
- [28] M. Ueda, *Nat. Rev. Phys.* **2**, 669 (2020).
- [29] M. Kastner, *Phys. Rev. Lett.* **106**, 130601 (2011).
- [30] P. Jurcevic, B. P. Lanyon, P. Hauke, C. Hempel, P. Zoller, R. Blatt, and C. F. Roos, *Cah. Rev. The.* **511**, 202 (2014).
- [31] M. Block, Y. Bao, S. Choi, E. Altman, and N. Y. Yao, *Phys. Rev. Lett.* **128**, 010604 (2022).
- [32] T. Minato, K. Sugimoto, T. Kuwahara, and K. Saito, *Phys. Rev. Lett.* **128**, 010603 (2022).
- [33] D. Lynden-Bell and R. M. Lynden-Bell, *Mon. Not. R. Astron. Soc.* **181**, 405 (1977).
- [34] W. Thirring, *Z. Phys. A: Hadrons Nucl.* **235**, 339 (1970).
- [35] W. Thirring, H. Narnhofer, and H. A. Posch, *Phys. Rev. Lett.* **91**, 130601 (2003).
- [36] M. K.-H. Kiessling and T. Neukirch, *Proc. Natl. Acad. Sci. USA* **100**, 1510 (2003).
- [37] J. Barre, D. Mukamel, and S. Ruffo, *Phys. Rev. Lett.* **87**, 030601 (2001).
- [38] V. Latora, A. Rapisarda, and C. Tsallis, *Phys. Rev. E* **64**, 056134 (2001).
- [39] V. Latora, A. Rapisarda, and C. Tsallis, *Physica A* **305**, 129 (2002).
- [40] C. Tsallis, *Introduction to Nonextensive Statistical Mechanics* (Springer, New York, 2009).
- [41] M. Antoni and S. Ruffo, *Phys. Rev. E* **52**, 2361 (1995).
- [42] D. Mukamel, S. Ruffo, and N. Schreiber, *Phys. Rev. Lett.* **95**, 240604 (2005).
- [43] R. Bachelard and M. Kastner, *Phys. Rev. Lett.* **110**, 170603 (2013).
- [44] M. Joyce, J. Morand, F. Sicard, and P. Viot, *Phys. Rev. Lett.* **112**, 070602 (2014).
- [45] N. Defenu, *Proc. Natl. Acad. Sci. USA* **118**, e2101785118 (2021).
- [46] D. Bagchi, *Phys. Rev. E* **95**, 032102 (2017).
- [47] P. Di Cintio, S. Iubini, S. Lepri, and R. Livi, *J. Phys. A: Math. Theor.* **52**, 274001 (2019).
- [48] S. Iubini, P. Di Cintio, S. Lepri, R. Livi, and L. Casetti, *Phys. Rev. E* **97**, 032102 (2018).
- [49] S. Tamaki and K. Saito, *Phys. Rev. E* **101**, 042118 (2020).
- [50] J. J. Wang, S. V. Dmitriev, and D. X. Xiong, *Phys. Rev. Res.* **2**, 013179 (2020).
- [51] D. Bagchi, *Phys. Rev. E* **104**, 054108 (2021).
- [52] T. M. Rocha Filho and R. Bachelard, *Phys. Rev. E* **100**, 042123 (2019).
- [53] S. Flach, *Phys. Rev. E* **58**, R4116 (1998).
- [54] V. E. Tarasov and G. M. Zaslavsky, *Commun. Nonlinear Sci. Numer. Simul.* **11**, 885 (2006).
- [55] H. Christodoulidi, C. Tsallis, and T. Bountis, *Europhys. Lett.* **108**, 40006 (2014).
- [56] G. Miloshevich, J. P. Nguenang, T. Dauxois, R. Khomeriki, and S. Ruffo, *Phys. Rev. E* **91**, 032927 (2015).
- [57] D. Bagchi and C. Tsallis, *Physica A* **491**, 869 (2018).
- [58] C. Anteneodo and C. Tsallis, *Phys. Rev. Lett.* **80**, 5313 (1998).
- [59] H. Christodoulidi, T. Bountis, C. Tsallis, and L. Drossos, *J. Stat. Mech.* (2016) 123206.
- [60] D. Bagchi and C. Tsallis, *Phys. Rev. E* **93**, 062213 (2016).